J. Condensed Matter Nucl. Sci. 14 (2014) 50–60

Research Article

Transient Vacancy Phase States in Palladium after High Dose-rate Electron Beam Irradiation

Mitchell Swartz *

JET Energy Inc., Wellesley Hills, MA, USA

Peter L. Hagelstein

Massachusetts Institute of Technology, Cambridge, MA, USA

Abstract

A high voltage electron irradiator was used to generate high vacancy content VP metal samples. High Frenkel defects (FD) content (vacancy phase) metal samples of Pd and Ni were generated by a single treatment with a high voltage electron irradiator (2.5 MV electrons, 2500 Gray/s dose rate, single portal, 1.50–3.0 megaGray midplane dose) at room temperature. These irradiation-synthesized, vacancy-phase (ISVP) metals were examined for their room-temperature annealing rate using four-terminal conductivity measurements. We show that high dose rate supervoltage irradiated palladium and nickel can achieve saturation densities of defects at the level of a few tenths percent and that level can be followed with the appearance of lattice quakes repairing the damage. The most heavily irradiated samples developed incremental electrical resistivities of $\sim$4 $\mu\Omega$-cm, with rapid recovery consistent with room-temperature annealing. The early labile vacancy phase state of ISVP metals has a half-life $\sim$2.5 h. Lattice quakes are observed when electrical transconduction spectroscopy is used to monitor the lattice healing and vacancy recombination. The irradiation produced an effective increase in the cross-sectional area of the palladium wires (99.98%) pure) of $\sim$2.5% at 3 megaGray delivered, consistent with the literature.
 ISSN 2227-3123

Keywords: CF materials, Electrode Irradiation, Fukai states, Superabundant vacancies, Vacancy phase metals

1. Introduction – Frenkel Defects and Lattice Vacancies

1.1. Frenkel defects

A Frenkel defect (FD) (each a paired entity) is a lattice "hole" AND its counter-defect which is simultaneously produced when an atom jumps from its normal position to an interstitial site, such as secondary to bombardment from a high energy incident neutron, electron, or other particle [1]. Frenkel defects must be distinguished from Schottky defects where atoms move to the grain boundaries, and surfaces, leaving the vacancies far behind.

*E-mail: mica@theworld.com

 ISSN 2227-3123

Why are Frenkel defects (FD) important to cold fusion and lattice-assisted nuclear reactions (LANR)? FD are important to excess enthalpy reactions (CF or LANR) because they create empty lattice sites which are possibly nuclear active sites for the desired reactions. In addition, they can be stabilized by hydrogen atoms in the metal lattice, and – on some occasions – the FD themselves can become further ordered, and that too may also play a role in CF/LANR. For example, requisite deuterons, or their clusters, could enter the sites [2–5], including by Anderson focusing [5].

Furthermore, FD aggregation may be a *second sine qua non* for the success of excess enthalpy reactions in hydrogen (and deuteron) loaded metals – after high loading. As is now known, full loading of metals such as palladium with deuterons is the first *sine qua non* [6–8] but insufficient for the reactions which generate excess enthalpy; there is also required a time period of weeks [9]. One hypothesis suggested at ICCF-10 is that FD are diffusing into the metal lattice, and that diffusion is the reason for the long wait before the appearance of the desired excess enthalpy reactions. One relationship to CF/LANR is that up to several (perhaps 6) deuterons (10) can be associated with each FD, and they selectively enter the defects during deuteron flow producing critically required effects before the desired reactions appear [5]. Figure 1 shows the FD (vacancy) density, and electrical resistivity ($\mu\Omega$-cm).

These values are plotted in two dimensions both as a function of time and delivered dose. Shown are the FD Density and ρ for theoretically "pure" palladium, what was actually measured in the control specimen, and what was observed for irradiated Pd specimens (ISVP) to which 1.5 and 3.0 megaGray dose were delivered.

Paired FD (vacancies) in pure metals are well known, but are transient and recombine rapidly, driven by the 1.5 eV released per combining defect pair. And so, FD are present in pure metals only at very low concentrations –

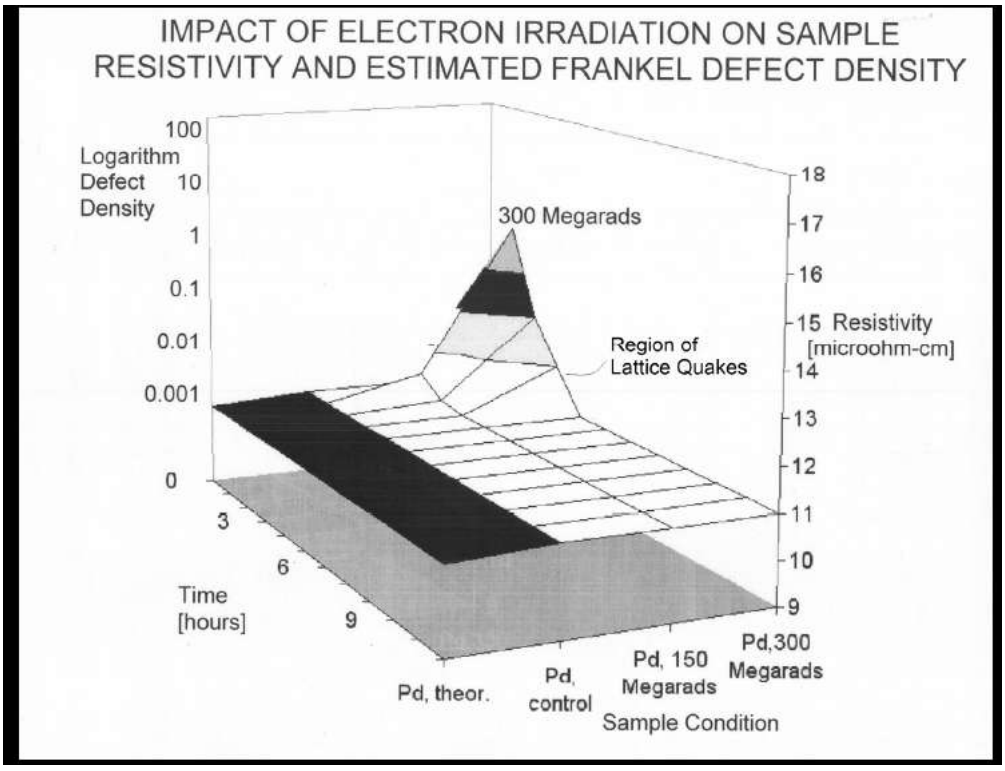

Figure 1. Frenkel Defect (vacancy) density, and electrical resistivity ($\mu\Omega$-cm).

Table 1. Some properties of irradiation-induced FD.

Enthalpy of formation	0.32 eV	Fukai
Number of hydrogen trapped in a vacancy	6 (for Pd)	Fukai
Diffusivity (cm^2/s)	10^8	
Theoretical max possible concentration	7.7%	Fecht (Fuk)
Peak achievable vacancies in Pd	18 at.%	Fuk
Remnant vacancies after annealing	1/3	
Specific incremental resistivities of some metals ρ_F ($\mu\Omega$-cm) per at.%		
Cu	1.3, 2.0	von Hippel, Ehrhart and Schlagheck
Al	3.9	Ehrhart and Schlagheck
Ag	1.5	von Hippel
Au	1.5	von Hippel
Ni	7.1	Bender and Ehrhart
Pd	900^{100}	

unless some procedure has specifically been used to generate them and if means are also provided to halt thermally driven recombination of such vacancies [11]. When formed, the Frenkel pair defects (often termed 'vacancies' or discomposition in the literature) are characterized by diffusivities and the induced specific electrical resistivities listed in Table 1.

Palladium hydrides have been long studied [12–16]. When FD defects are produced in large quantities in select Group VIII metals such as when hydrogen atoms (well known from the hydrides of such metals) stabilize them, the defects can, on occasion, form ordered clusters [17–20]. These were first noted in 1994, during X-ray diffraction studies, when Fukai [17,18] discovered that palladium lattices filled with hydrogen could undergo a irreversible lattice contraction at high temperatures into an ordered state, and one with characteristic features of vacancy formation. What was most interesting was that this new observed phase of matter had concentrations of vacancies (up to circa 30%) which were many orders of magnitude greater than had ever been seen previously. These ordered states of hydrides are, therefore, called super abundant vacancies (SAV) or Fukai states. Surprisingly, these HTHP FD have vacancies which are stable following outgassing of the hydrogen, and on occasion can be observed to form ordered clusters. Such high FD/vacancy state metals are referred to as vacancy phase (VP) materials. These include ordered vacancy phases and new types of lower density hydrided "pure" metals and alloys.

1.2. Vacancy phase metals

The generation of FD, and possible attainment of high levels of VP metals is reasonably well understood theoretically. In hydrogen loaded palladium, FD defects can exist a bit longer, stabilized by the electronic structure of the loaded PdH. Their existence is still limited by the vacancy diffusion rate and the very low production rate of vacancies. Hydrogen atoms and the FD stabilize each other by a few tenths of an eV per neighboring hydrogen. In NiH, a metal vacancy is energetically favored by $\sim$0.5 eV; in PdH by a few tenths of an eV. These numbers should be compared to the $\sim$1.5 eV formation energy required for FD (vacancy) creation in the pure metal. As a result of the stabilization, thermodynamics predicts that the number of hydrided metal lattice vacancies, which can exist in loaded NiH and PdH, can be limited by the vacancy diffusion rate and the production rate of vacancies [5]. The dynamics of such ordered cluster formation is complicated; and that includes because interstitials which can impede the clustering formation, and because other isotopes of hydrogen (H vs. D) can impede the loading.

Increased quantities of FD in metals can be generated by near-melting temperatures, by high temperature-high pressure systems [21] and by electron [5,17,18, 21–25] or neutron irradiation, and torsion [20]. The first (and easiest) method takes the metal just below the melting point to generate vacancies which are then frozen into position by

lowering the temperature. This procedure attains a maximum vacancy concentration of 0.1%. The FD production rate can be increased when metals are irradiated by a flux of high energy electrons. Metals irradiated with neutrons or supervoltage (>1.5 MV) electrons at high doses, and high dose rates, achieve a saturation density of defects that are a few tenths of a percent, and involving many modes of annealing. There is also much interest in the high temperature high pressure (HTHP) vacancy phase (VP) synthesis because of the observation of ∼25% metal FD in NiH and 18% in PdH developed by the anvil-presses on six sides of the samples [17].

Both the FD, the rarer clusters, and SAV which can form from them, are observable through their Huang anomalous scattering [26–29], and relatively strong small-angle X-ray scattering, respectively. Huang scattering [26] is the development of relatively wide angle diffuse scattering produced by the vacancies upon the very sharp diffraction peaks which characterize x-ray diffraction images of "pure" perfect crystals.

Previously, we briefly reported the presence of transient vacancy phase states [30] and the performance of vacancy phase nickel cathodes in ordinary water [31]. This paper reports further investigations which were made on electron-irradiation-induced metal lattice dislocations and vacancies in palladium. We use two units of irradiation here. The first is the dose delivered to the material, which is Gray (where 100 rads is one Gray). The second is the normalized fluence (flux) of electrons (number of electrons/cm^2) which actually generates that delivered dose.

2. Experimental: Materials and Methods

Palladium samples (wire, annealed post cold-drawn, lot "Z" (IMRA), Johnson Matthey (99.98%, nominal 1.0 mm diameter, 1 cm length, generally characterized with the 311 metal crystalline axis being perpendicular to the long axis of the wires) were used. To correct for geometric factors, the physical size of the wires were measured using a Sylvac caliper (Fowler Type Ultracal-III, Newton MA; spatial resolution 0.01 mm, accuracy 30 μm, precision 10 μm). The sample wires were measured, before and sequentially after irradiation, for diametric changes at 0, 45 and 90 degree angles along their entire length in the setup configuration. Thereafter, diametric measurements and four-terminal conductance measurements were used with the geometric sample factors to derive the semiquantitative electrical conductivity of the samples.

Dual Angle X-ray spectroscopic examination was performed on some of the palladium wire samples to determine the impact of loading pre-irradiation Spectroscopic curves were generated using a Cu anode, 300 mA, 60 kVp; 1/2 degree scatter slit, 1/2 degree divergence slit, Molybdenum vertical collimators, 0.15 mm receiving slit, dose rate ∼10 kiloGray per second, with a scan rate 0.25 degrees/min at 0.02 degree increments for fine structure determination.

To generate high vacancy content metal samples, a high voltage electron irradiator was used to produce damage for all experiments, except the controls. A van de Graaff was adjusted to deliver 2.5 MV electrons [32] at ultrahigh dose rate at the MIT High Voltage Research Laboratory (∼2500 Gray/s dose rate) with a single portal over 20 min to 1.5–3 megaGray midplane dose with the samples located approximately 7 cm from the horn. All samples were located within that peak cross-section of the incident beam. The irradiated wires were arranged on filter paper (Whatman #1, 9.0 cm) and irradiated perpendicular to their long axis. No rearrangement was used during irradiation, but half the samples were removed midway through the irradiation procedure. The wires were handled by their penultimate terminal segments, <1.5 mm). They were contained in polypropylene or polyethylene; and kept at room temperature, except during irradiation.

The presence of vacancies was qualitatively estimated through the changes observed by electrical resistivity measurements performed before and after irradiation. A significant increase in the resistivity was caused by the substantial defect production after the single dose irradiation, and thereafter the resistivity and sample area were examined, metachronously. (In contrast to synchronous, metachronous means later, after the event.)

The electrical conductivity was monitored by a four-terminal measurement (Keithly 225 current source, 610C electrometer). In control experiments determined that when sample input power exceeds 20 nW (∼3 nW for gold),

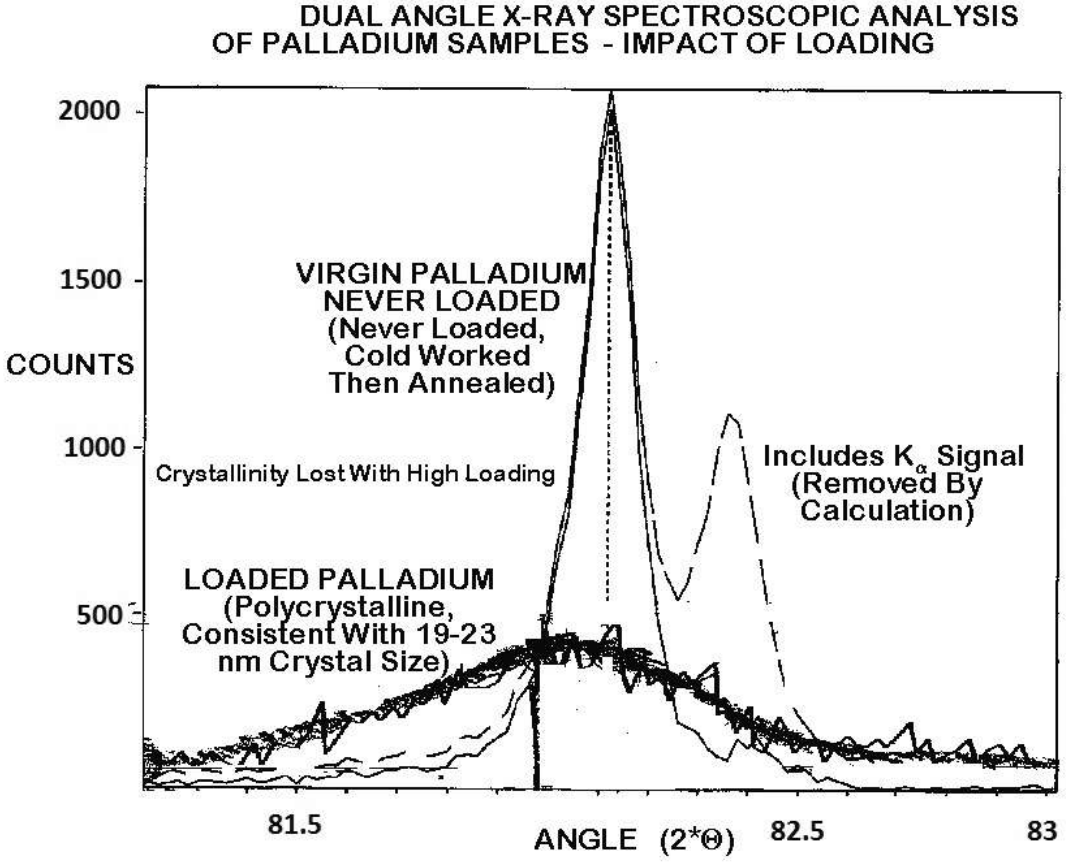

Figure 2. Dual angle X-ray spectroscopic examination of the of palladium wire.

there resulted a degree of electrical dissipation sufficient to generate stable electrical conduction measurements using this system. All measurements thereafter exceeded that minimum power dissipation.

3. Results

Figure 2 shows three X-ray spectroscopic curves for two palladium samples. They are a "virgin" palladium wire (prior to both loading with hydrogen and prior to irradiation), and a palladium wire after loading with hydrogen. The virgin control wire had been annealed and cold worked. The thin solid curves are for the virgin wire. The thin dashed curve is the raw data which includes both of the $K_{\alpha 1}$ and $K_{\alpha 2}$ peaks which are characteristic of the horizontal rocking system. These are corrected in the thin solid curves. The thicker and broader curve is the output of a hydrided (loaded to 0.95) palladium wire.

One result of this measurement was the corroboration that these palladium wires tended to have their crystallographic 311 vector perpendicular from the long axis of the palladium wire. Another result is that loading severely changed the lattice structure. All curves in Fig. 5 demonstrate the 311 characteristic peak (plotted as $2^*\theta$). Relatively,

this is especially true for the virgin palladium wire compared to the loaded wire. The virgin wires have much greater magnitude of the 311 peak.

Three X-ray spectroscopic curves are shown (300 mA, 60 kVp) as discussed in the text.

Figure 3 shows the diameter of palladium wires three days following a single irradiation dose. The size of the wire in millimeters is shown as a function of given dose. The results of eight (8) wires are shown. The range of thicknesses of palladium wires are shown three days after electron beam irradiation. The limits show the range of measurements (two standard deviations). Two given irradiation doses (1.5 and 3 megaGray) are shown, along with the controls (that is unirradiated or "virgin") palladium wire.

The palladium samples (nominally "1.0 mm") were ∼1.01 mm diameter, and their diameter increased with remnant structure damage for days following a single irradiation dose (Fig. 3). Their girth increased for those most highly irradiated samples to 1.02 mm. The produced effective increase in the cross-sectional area of the palladium wire (99.98% pure) was 0.75% at 1.5 megaGray, and was ∼2–2.5% at 3 megaGray delivered dose (standard deviation ∼10–20 μm).

The results of eight (8) different wires are shown. The range of thickness of palladium wires are shown three days after the single electron beam irradiation of all samples (nominally "1.0 mm").

By the use of area measurement here with the measured electrical resistance, a semi-quantitative correction for the irradiated wire electrical resistivities were derived (Figs. 1 and 2). Figure 4 shows the palladium wire electrical

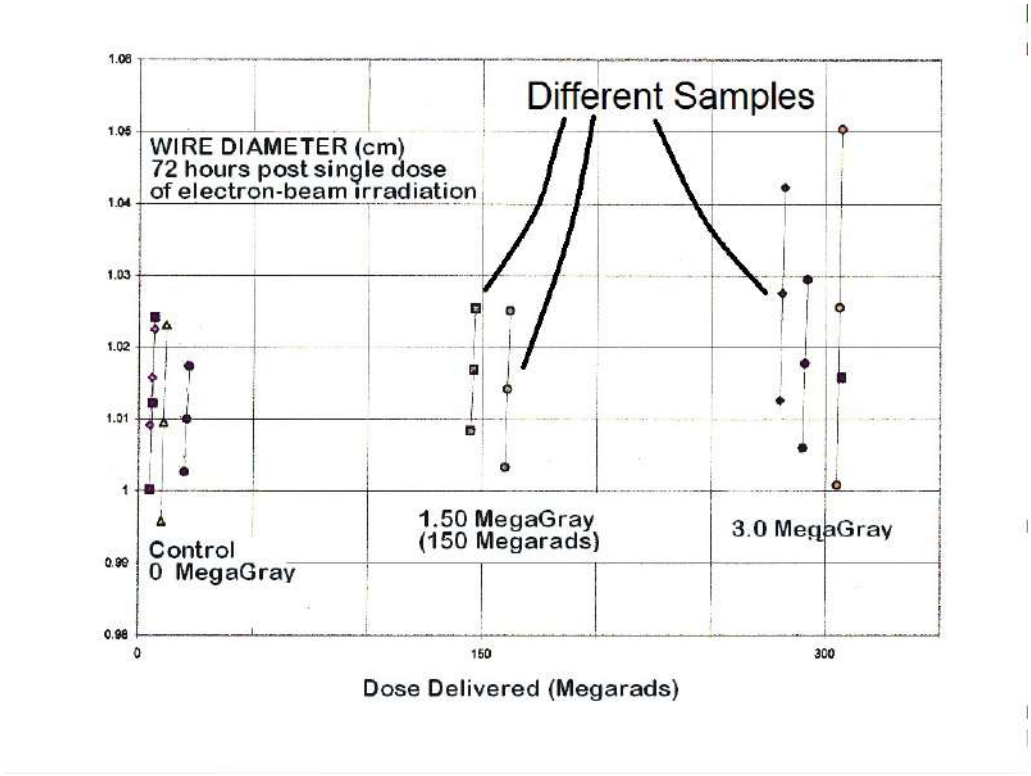

Figure 3. Palladium wire diameter three days after electron-beam irradiation-created vacancy states.

resistivity after its single-dose electron beam irradiation This curve shows the electrical resistivity of a palladium wire sample (99.99%) over time. At t = 0, the single dose electron beam irradiation occurred. The palladium sample received 3.0 megaGray midplane dose over twenty minutes. The electrical resistivity is compared with the theoretical expected resistivity of "pure" palladium.

The most heavily irradiated samples developed increased resistivities of as much as 4 $\mu\Omega$-cm. This fell off with a half-life of approximately 2–3 h, until by 6 h after irradiation the resistivity was approximately 11.5 $\mu\Omega$-cm (Fig. 4). There appear to be two distinct falloff regions of electrical resistivity, with final drift back toward the normal resistivity of virgin samples. Following the rapid falloff region shown in Fig. 1 with the half-life of 2.5 h is a region of slower resistivity falloff in the range of $2.4 \times 10^{-5}\mu\Omega$-cm/s (over circa a range of 6–9 h). This shows the post-irradiation, loss of Fukai state material over 20 min. The electrical resistivity of the virgin (unirradiated) Pd samples were approximately 1.01% greater than theoretically expected (expected 10.8 $\mu\Omega$-cm, measured 10.909). This resistivity of the samples postirradiation was time-dependent consistent with room-temperature annealing as shown in Figs. 1, 4 and 5.

The upper curve shows the electrical resistivity of a palladium wire sample (99.99%) over time before, and after

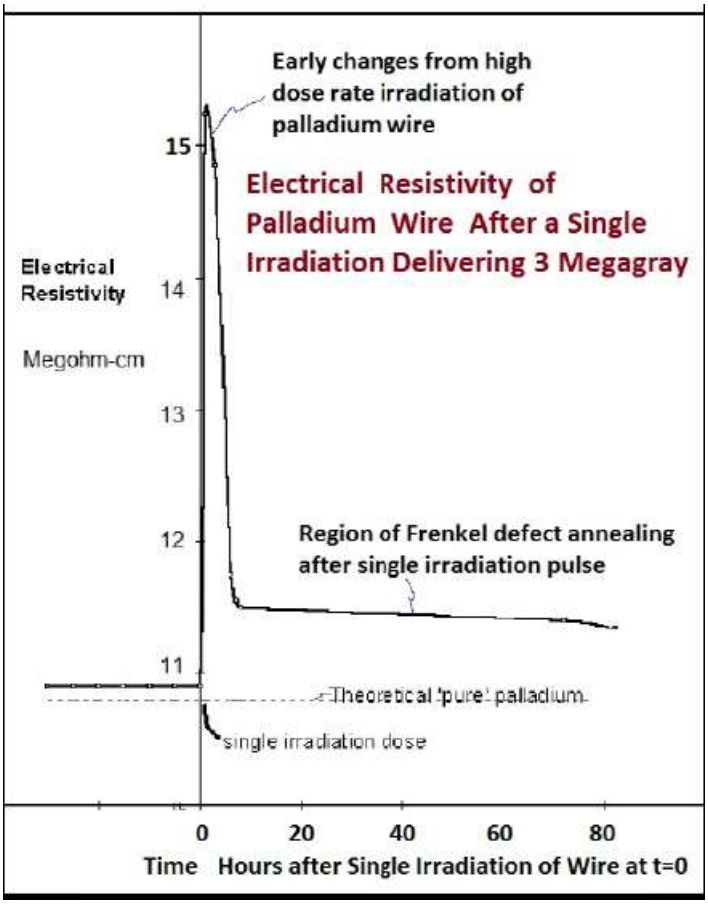

Figure 4. Palladium wire electrical resistivity post electron beam irradiation.

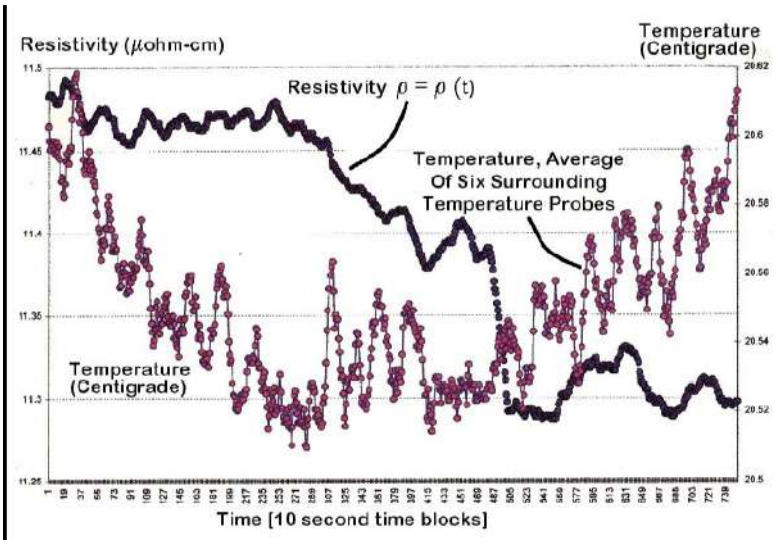

Figure 5. Fine structure of palladium sample resistivity as a function of time, following electron beam irradiation.

irradiation at $t = 0$. The palladium sample received 3.0 megaGray midplane dose over twenty minutes. The electrical resistivity is compared with the theoretical expected resistivity of "pure" palladium, which is the lower dashed curve.

Figure 5 shows the fine structure of a palladium sample's electrical resistivity following its electron beam irradiation. Of special interest are the lattice –quakes. In Fig. 5, two curves are shown. The upper, thicker, curve is the electrical resistivity of the sample over time (in 10 s time blocks) and demonstrates the fine-structure changes which occur during room-temperature annealing. The palladium wire sample received 3.0 megaGray. The second curve (solid dots) shows the average temperature of six thermocouple probes used to examine the immediate environment around the sample.

The upper, thick, curve is the electrical resistivity of the sample over time, in 10 s time blocks. The fine-structure changes are room-temperature annealing. The second lower curve (solid dots) shows the average temperature of six thermocouple probes used to examine the immediate environment around he sample.

4. Discussion and Interpretation

There exists major, yet significantly recoverable, effects wrought upon palladium wire samples following high dose-rate electron beam irradiation yielding large numbers of FD. High FD content (vacancy phase) metal samples were generated by a single treatment with a high voltage electron irradiator (2.5 MV electrons, 2500 Gray/s dose rate, single portal, 1.5–3.0 megaGray mid-plane dose) at room temperature, initially, and they were transient.

Irradiation produced an effective increase in the cross-sectional area of the palladium wires (99.98% pure) of 0.75% at 1.5 megaGray, and as much as 2–2.5% at 3.0 megaGray delivered dose, consistent with the literature. This finding of volumetric expansion of the irradiated wires is consistent with the literature because it is well known that irradiation of metals causes lattice site breakdown and that the creation of defects so wrought increases the volume (and in this case area).

The most heavily irradiated samples developed incremental resistivities of $\sim$4 $\mu\Omega$-cm (virgin unirradiated sample resistivities and theoretical resistivities of 10.9 and 10.8 $\mu\Omega$-cm). This electrical resistivity of the samples, post-

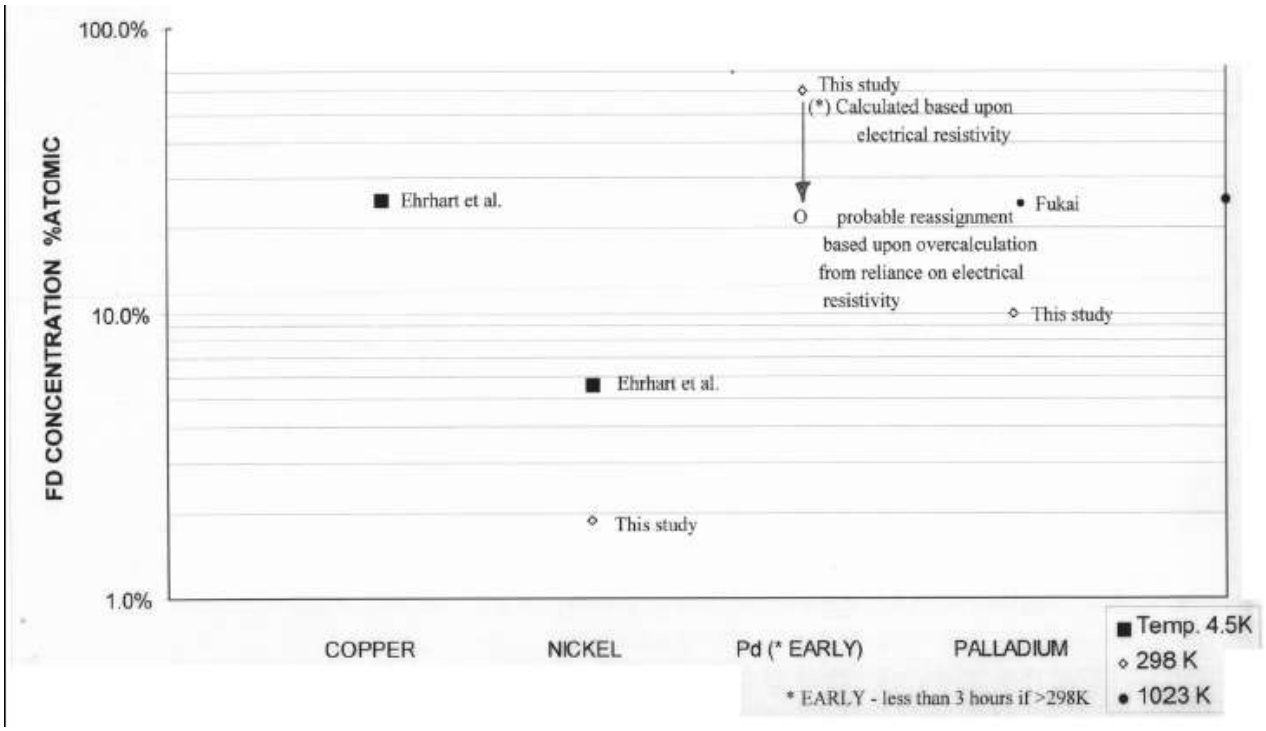

Figure 6. Induced incremental derived FD concentrations in palladium and other metals.

irradiation, was time-dependent, consistent with room-temperature annealing. In palladium, post 3 megaGray, after the rapid early falloff (half-life ∼2.5 h) there is a region of fewer induced FD and a much slower resistivity falloff ($\sim 2.4 \times 10^{-5} \mu\Omega$-cm /s).

In palladium, we have separated the annealing of irradiation-induced vacancies into two phases of FD recombination and loss. The first has the possible appearance of a level of vacancies similar to those described by Fukai [17,18]. The latter short-lived phase occurs within hours and are levels consistent with the other electron irradiation reports [16, 21–25].

Lattice quakes are observed in the second region. The fine structure of the electrical resistivity (Fig. 5) shows that in intermediate time region, most observable at circa 7–9 h after the irradiation, there can be seen these complex dynamic structural changes.

Figure 6 plots from several experiments the induced incremental derived FD concentrations in palladium, and other metals, as both obtained by electron irradiation here, compared to the high temperature-high pressure (HTHP) system.

These are the incremental induced derived FD concentrations, for metals, obtained by electron irradiation. Here, results are compared to the high temperature-high pressure (HTHP) systems.

In these palladium samples, post high dose irradiation, based on the electrical resistivity changes, the calculated FD concentration (% atomic FD) within the first 3 h post-irradiation was in the range of ∼30–45%. We believe that this is an over-calculation based upon reliance on electrical resistivity; and that the more likely range obtained was ∼20–30%, similar to that reported by Fukai for palladium and by Ehrhart for copper.

In the longer term, the calculated FD concentration was in the range of 8–10%. The FD formation rate as function

of the electron irradiation flux is estimated at 10-60% atomic FD/coulombs/cm^2 within the first 3 h post-irradiation. In the longer metachronous post-irradiation period, this decreased to 7–10% atomic FD/coulombs/cm^2. These levels are greater by more than orders of magnitude than those observed for copper and nickel [25].

By contrast, in nickel, electron bombardment by 3 MeV leads to vacancy concentrations of 0.0003-0.0007 for 1–2 $\times$ 10^{18} electrons/cm^2, with a defect saturation of about 0.0018. These nickel control experiments produced short-lived defects, fewer in number than those left frozen in at 4.5 K.

5. Conclusion and Summary

In summary, electron irradiation offers opportunity for larger levels of defects than that achieved by other methods. FDs, and ordered vacancy phase (VP) solids loaded with FDs, may be important because they offer new materials with novel properties arising because of stabilizing hydrogen atoms offering a few tenths of an eV per neighboring hydrogen.

From a materials point of view, one important impact of these findings is that by electron-irradiating Group VIII metals, there may be opportunity for obtaining larger concentrations of FD than achieved by other methods. Competing kinematics, and other metallurgical issues, make producing large amounts of such defects (vacancy phase metals) quite difficult. However, metals loaded with hydrogen, such as deuterium in palladium, can change all that.

Another implication is also that electrical transconduction spectroscopy, normally used to monitor hydride loading in the Group VIII metals, can also examine the lattice healing and vacancy recombination, through these lattice-quakes.

Another impact of this work is that, looking forward, wire diameter should be considered during electron beam irradiation or hydrogen loading so as to further supplement and correct Archemedic estimations and X-ray spectroscopic deduction of the loading. Specifically, correction for geometric factors to determine the electrical resistivity will improve loading determinations based on the variation of resistance for the b phase palladium following loading with deuterons [33]. Electrical resistivity, rather than electrical resistance, may be more important because it is indicative of material composition by removal of the geometric factors. Although X-ray spectroscopy can be used to evaluate lattice spacing, samples should be physically followed thereafter to correct for their changing geometric size.

Acknowledgment

The authors acknowledge and thank JET Energy, Inc. for support of this work, and to Gayle Verner and Dr. Alex Frank for their very helpful comments. The authors are also grateful to J.Adario at MIT who performed x-ray spectroscopy, Kenneth Wright of MIT HVRL for meticulous engineering of the irradiation, Michael McKubre and Fran Tanzella for loading the Pd sample, and the Department of Electrical Engineering and DARPA for support at MIT.

References

[1] A. von Hippel, Molecular Science and Molecular Engineering, MIT Press, Cambridge, USA, 1959.
[2] G. Miley, X. Yang and H. Hora, Ultra-high density deuteron-cluster electrode for low-energy nuclear reactions, *J. Condensed Matter Nucl. Sci.* **4** (2011) 256–268.
[3] P. Tripodi, N. Armanet, V. Asarisi, A. Avveduto, A. Marmigi, J.D. Vinko, J. Biberian, The effect of hydrogenation/dehydrogenation cycles on palladium physical properties, *Phys. Lett. A* **373** (2009) 3101–3108.
[4] P. Tripodi, N. Armanet, V. Asarisi, A. Avveduto, A. Marmigi, J. Biberian, J.D. Vinko, The effect of hydrogen stoichiometry on palladium strain and resistivity, *Phys. Lett. A* **373** (2009) 4301–4306.
[5] M. Swartz, Catastrophic active medium hypothesis of cold fusion, *Proc. Fourth International Conference on Cold Fusion*, Vol. 4, sponsored by EPRI and the Off. Naval Research, 1994.

[6] A. Takahashi and N. Yabuuchi, Study on 4D/TSC condensation motion by non-linear Langevin Equation, American Chemical Society LENRSB1, 57–83, 2008; A Takahashi, Physics of Cold Fusion by TSC Theory, *J. Physical Science and Application* **3**(3) (2013) 191–198.
[7] M. McKubre, F. Tanzella, P. Hagelstein, K. Mullican and M. Trevithick, The need for triggering in cold fusion reactions, *Proc. ICCF-10*, Cambridge, MA, 2003.
[8] M. Swartz, Survey of the observed excess energy and emissions in lattice assisted nuclear reactions, *J. Scientific Exploration* **23**(4) (2009) 419–436.
[9] M.R. Swartz, Phusons in nuclear reactions in solids, *Fusion Technol.* **31** (1997) 228–236.
[10] M.R. Swartz and G. Verner, Excess heat from low electrical conductivity heavy water spiral-wound Pd/$D_2$0/Pt and Pd/$D_2$0-P$dC1_2$/Pt Devices, *ICCF-10*, Cambridge, MA, 2003.
[11] P. Hagelstein and M. Swartz, Optics and Quantum Electronics, *MIT RLE Progress Report* **139** (1) (1997) 1–13.
[12] B. Baranowski, *Plat. Met. Rev.* **16** (1972) 10.
[13] A.W. Szafranski, *Phys. Status Solidi* (A) **19** (1973) 459.
[14] F.A. Lewis, *The Palladium Hydrogen System*, Academic Press, London, 1967.
[15] A.W. Szafranski and B. Baranowski, *Phys. Status Solidi* (A) **9** (1972) 435.
[16] B. Baranowski and R. Wisniewski, *Phys. Status Solidi* **35** (1969) 593.
[17] Fukai and N. Okuma, Formation of superabundant vacancies in Pd hydride under high hydrogen pressures, *Phys. Rev. Lett.* **73** (1994) 1640.
[18] Fukai, Formation of superabundant vacancies in metal hydrides at high temperatures, *J. Alloys & Compounds* **231** (1995) 35–40 .
[19] Zhang and C.A. Alavi, First principles study of superabundant vacancy formation in metal hydrides, *J. Am. Chem Soc.* **127** (2005) 9868–9817.
[20] M. Krystian, D. Setman et al., Formation of superabundant vacancies in nano PdH generated by high pressure torsion, *Scripta Materialia* **62** (2010) 49–52.
[21] P. Ehrhart and U. Schlagheck, Investigation of Frenkel defects in electron irradiated copper by Huang scattering of X-rays, *J Phys. F: Metal Phys.* **4** (1974) 1575–1587.
[22] P. Ehrhart, Diffuse X-ray scattering studies of neuron- and electron-irradiated Ni, Cu and dilute alloys, *Philosophical Mag. A* **60 3** (1989) 283–306.
[23] P. Ehrhart and W. Schilling, Investigation of interstitials in electron irradiated aluminum by diffuse X-ray scattering experiments, *Phys. Rev B* **8**(6) (1973) 2604–2621.
[24] O. Bender and P. Ehrhart, Self-interstitital atoms, vacancies, and their agglomerates in electron-irradiated nickel investigated by diffuse scattering of X-rays, *J. Phys. F: Metal Phys.* **13** (1983) 911928.
[25] P. Ehrhart, Investigation of radiation damage by X-ray diffraction, *J. Nuclear Materials* **216** (1994) 170–198.
[26] K. Huang, X-ray reflexions from dilute solid solutions, *Proc. Roy. Soc*. **A190** (1947) 102–117.
[27] R.I. Barabash, J.S. Chung and M.F. Thorpe, Lattice and continuum theories of Huang scattering, *J. Phys.: Condens. Matter* **11** (1999) 3075–3090.
[28] P.R. Dederichs, The theory of diffuse X-ray scattering and its application to the study of point defects and their clusters, *J. Phys. F: Metal Phys.* **3** (1973) 471–496.
[29] P. Ehrhart and H. Trinkaus, Diffuse scattering from dislocation loops,*Phys. Rev. B* **25** (2) (1982) 834.
[30] M. Swartz, P.L. Hagelstein, G. Verner and K. Wright, Possible transient vacancy phase states, Abstract *ICCF-7 in The Seventh Int. Conference on Cold Fusion*, Vancouver, Canada, 1998.
[31] M. Swartz, P.L. Hagelstein, G. Verner and K. Wright, Vacancy phase nickel cathodes, Abstract *ICCF-8, in 8th International Conference on Cold Fusion*, Lerici (La Spezia), Italy: Italian Physical Society, Bologna, Italy, 2000.
[32] N. duV. Tapley, *Clinical Applications of Electron Beam,* Wiley, NY, 1976.
[33] S. Crouch-Baker, M.C.H. McKubre and F.L. Tanzella, Variation of Resistance with Composition in the b-Phase of the H–Pd System at 298 K, *Zeitschrift fur Physikalische Chemie, Bd.* **204**(S)(1998) 247–254.